Motion planning for an elastic Kirchhoff plate

Motion planning for an elastic Kirchhoff plate

J. Schröck, T. Meurer, and A. Kugi

***Abstract*— The motion planning problem is considered for a cantilevered orthotropic Kirchhoff plate with spatially varying coefficients and distributed piezoelectric patch actuators. For this, the spectral representation of the corresponding equations of motion is utilized to systematically construct a flatness-based parametrization of state and inputs. These enable a very intuitive motion planning to realize prescribed high-speed rest-to-rest motions as is illustrated in simulation scenarios.**

I. Introduction

In many technical fields, researchers try to learn from nature to improve system performance and efficiency. While most technical machinery represent multi-body systems typically consisting of several rigid parts connected by moveable links, objects in nature extensively utilize flexible elastic structures, which allow a direct adaptation of their shape and orientation. In order to imitate this concept, in recent years, the development of so-called smart structures, i.e. elastic materials with integrated actuators and sensors, has received significant attention. Selected applications in particular comprise adaptive optics, flow control as well as adaptive wing structures.

Motivated by these ideas, we subsequently address the realization of a transient elastic deformation of a 2-dimensional flexible structure. In particular, the benchmark example of a cantilevered plate is considered, which is actuated by a finite number of spatially distributed patch actuators, see Figure 1. The considered motion planning and feedforward control problem thereby concerns the realization of high-speed rest-to-rest transitions between different desired deflection profiles. Our solution approach directly exploits the infinite-dimensional system dynamics in terms of the Kirchhoff plate equation. The governing partial differential equation (PDE) includes spatially varying coefficients to cover local damping and stiffening effects arising from spatially distributed actuators.

For motion planning and feedforward control of finite-dimensional systems, differential flatness [5] is a widely approved concept. A system is called differentially flat if all system states and inputs can be parametrized by a so-called flat or basic output and its time-derivatives up to a certain problem dependent order. In recent years, significant progress has been made for the extension of the flatness concept to systems governed by PDEs. For flexible structures, selected examples address Euler-Bernoulli and Timoshenko beam models [6], [2], [15] as well as circular Kirchhoff plate models [17]. Given rectangular plate geometries with constant coefficients [13], [16] proposes a projection–based design under the assumption of an infinite-dimensional system input, which is approximated by a finite number of distributed actuators.

In the present contribution, a general approach for the flatness-based solution of the motion planning and feedforward control problem is presented for 2-dimensional flexible structures. Based on the spectral representation of the Kirchhoff plate model the state and input parametrization are systematically constructed in the operational domain in terms of Weierstrass canonical products, which correspond to differential operators of infinite order in the time domain. Their convergence is briefly analyzed and a graphical convergence indicator is introduced together with an efficient realization of the feedforward controller by making use of a weighted-residual approach. With this, very intuitive motion planning is developed to track prescribed rest-to-rest transitions. The tracking performance is studied in simulation scenarios for the realization of highly transient spatial-temporal desired trajectories for the plate deflection.

The paper is organized as follows: Section II introduces the motion planning problem for a cantilevered Kirchhoff plate. The weak formulation and the resulting spectral plate representation are derived in Section III. The latter serves as the basis for the proposed design approach presented in Section IV. Finally, simulation results shown in Section V illustrate the tracking performance.

II. Motion planning problem

In the following, motion planning is considered for a damped cantilevered orthotropic Kirchhoff plate (see Figure 1) governed by the PDE

$$\rho\partial_t^2 w + \gamma\partial_t w + \partial_{x^1}^2(I_1\partial_{x^1}^2 w) + \partial_{x^2}^2(I_2\partial_{x^2}^2 w) + \nabla^2(I_3\nabla^2 w) + \partial_{x^1}\partial_{x^2}(I_4\partial_{x^1}\partial_{x^2} w) = -\sum_{k=1}^{N_p}\Gamma_k u_k \quad (1)$$

Here, $\nabla^2 = \partial_{x^1}^2 + \partial_{x^2}^2$, $w(x^1, x^2, t)$ is the deflection, and $\rho(x^1, x^2)$, $\gamma(x^1, x^2)$, $I_j(x^1, x^2) > 0$, $j = 1, ..., 4$ denote mass per unit area, viscous damping, and flexural rigidity, respectively, with $(x^1, x^2) \in \Omega_c = [0, L^1] \times [0, L^2]$. Spatially varying coefficients arise from the structural contributions of N_p piezoelectric patch actuator pairs (each consisting of two individual patches mounted symmetrically on the upper and lower plate surface) in terms of spatial characteristics represented by $\Lambda_k(x^1, x^2)$ (cf. Figure 1). In particular we have $\rho(x^1, x^2) = \rho^c + 2\sum_{k=1}^{N_p}\Lambda_k(x^1, x^2)\rho_k^p$, $\gamma(x^1, x^2) = \gamma^c + 2\sum_{k=1}^{N_p}\Lambda_k(x^1, x^2)\gamma_k^p$, and $I_j(x^1, x^2) =$

J. Schröck, T. Meurer, and A. Kugi are with the Automation and Control Institute (ACIN), Vienna University of Technology, Gußhausstr. 27–29, 1040 Vienna, Austria, meurer@acin.tuwien.ac.at

Post-print version of the article: J. Schröck, T. Meurer, and A. Kugi, "Motion planning for an elastic Kirchhoff plate", in *Proceedings of the American Control Conference (ACC)*, Montreal, Canada, Jun. 2012, pp. 652–657
The content of this post-print version is identical to the published paper but without the publisher's final layout or copy editing.

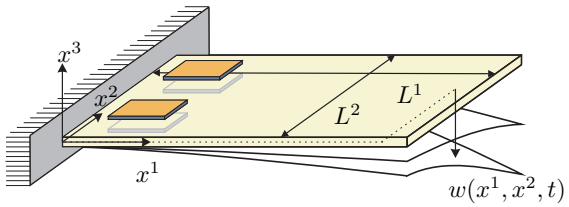

Fig. 1: Schematics of the patch-actuated plate.

$I_j^c + 2\sum_{k=1}^{N_p} \Lambda_k(x^1,x^2) I_{j,k}^p$ with superscripts c and p referring to the carrier and patch material (see, e.g., [1]). In addition, we have $\Gamma_k(x^1,x^2) = \Gamma_k^p[a_1^{11}\partial_{x^1}^2\Lambda_k(x^1,x^2) + a_1^{22}\partial_{x^2}^2\Lambda_k(x^1,x^2)]$ with a_1^{11}, a_1^{22} referring to the actuator material and Γ_k^p summarizing remaining parameters of the actuators. The respective geometric and natural boundary conditions for the cantilevered plate are given by

$$w = \partial_{x^1} w = 0, \qquad x^1 = 0 \tag{2a}$$

$$\left.\begin{array}{l} I_n \partial_{x^n}^2 w + I_3 \nabla^2 w = 0 \\ \partial_{x^n}(I_n \partial_{x^n}^2 w) \\ \quad + \partial_{x^n}(I_3 \nabla^2 w + I_4 \partial_{x^\tau}^2 w) = 0 \end{array}\right\} \quad \begin{array}{l} x^1 = L^1 \vee \\ x^2 \in \{0, L^2\} \end{array} \tag{2b}$$

with $\nabla^2 = \partial_{x^n}^2 + \partial_{x^\tau}^2$, where n and τ refer to the normal and the tangential component of the boundary $\partial\Omega_c$. Zero initial conditions are assumed such that $w(x^1,x^2,0) = \partial_t w(x^1,x^2,0) = 0$. The deflection at N_y reference locations on the plate is considered as system output, i.e.

$$y_i = w|_{(x^1,x^2)=(x_i^1,x_i^2)}, \quad i = 1,\dots,N_y. \tag{3}$$

With these preparations, the considered motion planning problem concerns the design of the feedforward control $\boldsymbol{u}^d(t) = [u_1^d(t),\dots,u_{N_p}^d(t)]^T$ to realize desired trajectories $t \mapsto \boldsymbol{y}^d(t) = [y_1^d(t),\dots,y_{N_y}^d(t)]^T$ for the system output $\boldsymbol{y}(t) = [y_1(t),\dots,y_{N_y}(t)]^T$ within prescribed time intervals. This in particular covers finite time transitions between steady state deflection profiles (rest-to-rest motion).

III. Weak formulation and spectral representation

The strong form (1), (2) of the equations of motion holds only if $\Lambda_k(x^1,x^2)$, $k = 1,\dots,N_p$ are sufficiently smooth. Nevertheless, to address more general situations, subsequently the mathematical model is considered in a weak sense. The weak form can be at first utilized to determine the spectral system representation, which serves as the basis for the proposed approach. Secondly, it enables an efficient realization of the controller by means of a finite-dimensional weighted-residual approximation.

A. Weak form of the equations of motion

Let $\mathcal{V} = H_C^2(\Omega_c) := \{w \in H^2(\Omega_c) \mid w(0,x^2) = \partial_{x^1} w(0,x^2) = 0\}$ and let $\mathcal{H} = L^2(\Omega_c)$ such that the inner product on $\mathcal{H}$ is given by

$$\langle \zeta^1, \zeta^2 \rangle_{\mathcal{H}} = \int_{\Omega_c} \rho \zeta^1 \overline{\zeta^2} \mathrm{d}x^1 \mathrm{d}x^2$$

for any $\zeta^1(x^1,x^2), \zeta^2(x^1,x^2) \in \mathcal{H}$. Multiplying (1) with a suitable test function $\zeta(x^1,x^2) \in \mathcal{V}$ and integrating[1] over the domain Ω_c taking into account the boundary conditions (2) yields the weak formulation

$$\begin{aligned} \langle \partial_t^2 w, \zeta \rangle_{\mathcal{H}} + \sigma_1(w,\zeta) + \sigma_2(\partial_t w, \zeta) \\ = -\sum_{k=1}^{N_p} \langle u_k \Gamma_k^p \Lambda_k/\rho, a_1^{11}\partial_{x^1}^2\zeta + a_1^{22}\partial_{x^2}^2\zeta \rangle_{\mathcal{H}} \end{aligned} \tag{4}$$

with

$$\begin{aligned} \sigma_1(\zeta^1,\zeta^2) = \int_{\Omega_c} \big[& I_1 \partial_{x^1}^2 \zeta^1 \overline{\partial_{x^1}^2 \zeta^2} + I_2 \partial_{x^2}^2 \zeta^1 \overline{\partial_{x^2}^2 \zeta^2} \\ & + I_3 \nabla^2 \zeta^1 \overline{\nabla^2 \zeta^2} + I_4 \partial_{x^1}\partial_{x^2} \zeta^1 \overline{\partial_{x^1}\partial_{x^2}\zeta^2} \big] \mathrm{d}x^1 \mathrm{d}x^2 \\ \sigma_2(\zeta^1,\zeta^2) = \int_{\Omega_c} \gamma \zeta^1 \overline{\zeta^2} \, \mathrm{d}x^1 \mathrm{d}x^2. & \end{aligned}$$

It can be shown that $\sigma_1(\cdot,\cdot)$ and $\sigma_2(\cdot,\cdot)$ represent symmetric sesquilinear forms, where $\sigma_1(\cdot,\cdot) : \mathcal{V} \times \mathcal{V} \to \mathbb{R}$ is $\mathcal{V}$-elliptic and $\sigma_2(\cdot,\cdot) : \mathcal{H} \times \mathcal{H} \to \mathbb{R}$ is $\mathcal{H}$-elliptic. In addition, the spaces $\mathcal{V}$ and $\mathcal{H}$ form a Gelfand triple $\mathcal{V} \hookrightarrow \mathcal{H} = \mathcal{H}' \hookrightarrow \mathcal{V}'$ with the pivot space $\mathcal{H} = \mathcal{H}'$ (here $\mathcal{V}'$ and $\mathcal{H}'$ denote the respective dual spaces). Hence, the duality pairing $\langle \cdot,\cdot \rangle_{\mathcal{V}',\mathcal{V}}$ can be considered as the continuous extension of $\langle \cdot,\cdot \rangle_{\mathcal{H}}$ on $\mathcal{V}' \times \mathcal{V}$. By the Lax-Milgram theorem, this implies the existence of invertible linear operators $\mathcal{A}_j$ defined as $\sigma_j(\zeta^1,\zeta^2) = \langle \mathcal{A}_j \zeta^1, \zeta^2 \rangle_{\mathcal{H}}$, $j = 1,2$. As is shown, e.g., in [1], these operators allow to interpret (4) as an abstract differential equation in $\mathcal{V}'$, i.e.

$$\partial_t^2 w + \mathcal{A}_1 w + \mathcal{A}_2 \partial_t w = \sum_{k=1}^{N_p} b_k u_k, \tag{5}$$

with $b_k u_k(t) \in L^2_{loc}([0,\infty); \mathcal{V}')$ given by

$$\langle b_k u_k, \zeta \rangle_{\mathcal{V}',\mathcal{V}} = \langle u_k \Gamma_k^p \Lambda_k/\rho, a_1^{11}\partial_{x^1}^2\zeta + a_1^{22}\partial_{x^2}^2\zeta \rangle_{\mathcal{H}}. \tag{6}$$

With these preparations, existence and uniqueness of a solution $w(x^1,x^2,t)$ can be guaranteed by [1, Thm. 4.1] with regularity properties $w(x^1,x^2,t) \in L^2(0,T;\mathcal{V})$, $\partial_t w(x^1,x^2,t) \in L^2(0,T;\mathcal{H})$, and $\partial_t^2 w(x^1,x^2,t) \in L^2(0,T;\mathcal{V}')$.

The abstract differential equation (5) can be rewritten as a coupled system of first order equation in $\boldsymbol{\mathcal{V}}_1 = \mathcal{V}_1 \times \mathcal{V}_1$, where $\mathcal{V}_1$ equals $\mathcal{V}$ but with $\sigma_1(\cdot,\cdot)$ as inner product. Hence, let $\boldsymbol{w}(t) = [w(\cdot,t), \partial_t w(\cdot,t)]^T$, then (5) implies

$$\partial_t \boldsymbol{w} = -\mathcal{A}\boldsymbol{w} + \sum_{k=1}^{N_p} \mathbf{b}_k u_k \tag{7}$$

with $\mathbf{b}_k = [0, b_k]^T$ and $-\mathcal{A} \in \mathcal{L}(\boldsymbol{\mathcal{V}}_1, \boldsymbol{\mathcal{V}}_1')$ defined as

$$-\mathcal{A}\boldsymbol{w} = \begin{bmatrix} 0 & \mathcal{I} \\ -\mathcal{A}_1 & -\mathcal{A}_2 \end{bmatrix} \boldsymbol{w} \tag{8}$$

with identity operator $\mathcal{I}$. The operator $-\mathcal{A}$ is the infinitesimal generator of an analytic C_0-semigroup on $\boldsymbol{\mathcal{H}}_1 = \mathcal{V}_1 \times \mathcal{H}$ as well as on $\boldsymbol{\mathcal{H}} = \mathcal{V} \times \mathcal{H}$ [1, Thm. 4.8].

[1] This requires special attention due to the orientation of the domain Ω_c.

Post-print version of the article: J. Schröck, T. Meurer, and A. Kugi, "Motion planning for an elastic Kirchhoff plate", in *Proceedings of the American Control Conference (ACC)*, Montreal, Canada, Jun. 2012, pp. 652–657
The content of this post-print version is identical to the published paper but without the publisher's final layout or copy editing.

B. Spectral system representation

The weak form introduced above can be directly utilized to determine the spectral system representation. For this, it is necessary to analyze the eigenproblem $-\mathcal{A}\boldsymbol{\phi} = \lambda\boldsymbol{\phi}$. Contrary to cantilevered Euler-Bernoulli beam models with spatially varying coefficients (see, e.g., [7]) no analytic or asymptotic solutions to the eigenproblem are available for the considered cantilevered Kirchhoff plate model[2]. Hence, the following assumption is imposed.

Assumption 1: Let $-\mathcal{A}$ be as above. Then

(A1) $-\mathcal{A}$ is a Riesz-spectral operator in the sense of [8] with isolated point spectrum $(\lambda_n)_{n\in\mathbb{N}}$ and $\lambda_n \neq 0$, $\forall n \in \mathbb{N}$.

(A2) The algebraic and geometric multiplicity r_n^a and r_n^g of λ_n, $n \in \mathbb{N}$ coincide with $r_n^a < \infty$ and $\sup \Re(\lambda_n) < \infty$.

(A3) The generalized eigenvectors $((\boldsymbol{\phi}_{n_j})_{j=1,\dots,r_n^a})_{n\in\mathbb{N}}$ and $((\boldsymbol{\psi}_{n_j})_{j=1,\dots,r_n^a})_{n\in\mathbb{N}}$ of $-\mathcal{A}$ and its adjoint $(-\mathcal{A})^*$ form a biorthogonal Riesz basis for $\boldsymbol{\mathcal{H}}$.

With this, any $\boldsymbol{w}(t) \in \boldsymbol{\mathcal{H}}$ can be represented in terms of the Fourier series

$$\boldsymbol{w} = \sum_{n\in\mathbb{N}} \sum_{j=1}^{r_n^a} \langle \boldsymbol{w}, \boldsymbol{\psi}_{n_j}\rangle_{\boldsymbol{\mathcal{H}}} \boldsymbol{\phi}_{n_j}. \tag{9}$$

Moreover, for any $\lambda \in \varrho(-\mathcal{A})$ with $\varrho(-\mathcal{A})$ denoting the resolvent set of $-\mathcal{A}$ the resolvent operator $R(\lambda, -\mathcal{A}) = (\lambda\mathcal{I} - (-\mathcal{A}))^{-1}$ is given by

$$R(\lambda, -\mathcal{A}) = \sum_{n\in\mathbb{N}} \frac{1}{\lambda - \lambda_n} \sum_{j=1}^{r_n^a} \langle \cdot, \boldsymbol{\psi}_{n_j}\rangle_{\boldsymbol{\mathcal{H}}} \boldsymbol{\phi}_{n_j}. \tag{10}$$

Since $-\mathcal{A}$ is the infinitesimal generator of a C_0–semigroup taking the Laplace transform of (7) yields the spectral representation

$$\begin{aligned} \hat{\boldsymbol{w}} &= R(s, -\mathcal{A}) \sum_{k=1}^{N_p} \mathbf{b}_k \hat{u}_k \\ &= \sum_{n\in\mathbb{N}} \sum_{k=1}^{N_p} \frac{\hat{u}_k}{s - \lambda_n} \sum_{j=1}^{r_n^a} \langle \mathbf{b}_k, \boldsymbol{\psi}_{n_j}\rangle_{\boldsymbol{\mathcal{H}}} \boldsymbol{\phi}_{n_j} \end{aligned} \tag{11}$$

with $s \in \varrho(-\mathcal{A})$ the Laplace variable and $\hat{\boldsymbol{w}}(s)$ and $\hat{u}_k(s)$ the Laplace transforms of $\boldsymbol{w}(t)$ and $u_k(t)$, respectively.

Remark 1: It should be pointed out that the case $r_n^g < r_n^a$ can be treated in a way similar to the presentation above with additional terms arising from the resulting Jordan-like structure. However, this case is outside the scope of this contribution.

IV. Flatness-based motion planning and feedforward control design

The spectral representation (11) directly enables the introduction of a flat output parametrizing state and input to provide a particularly intuitive solution of the motion planning and feedforward control problem.

[2]Solutions do exist only for plates with special domains (e.g. circular or rectangular) or special boundary conditions, see, e.g., [9], [11].

A. Flatness-based system parametrization

The spectral representation (11) yields an equivalent formulation according to

$$\hat{\boldsymbol{w}} = -\sum_{n\in\mathbb{N}} \sum_{k=1}^{N_p} \frac{e^{\mathcal{F}(\frac{s}{\lambda_n}, g)} \hat{\mathcal{D}}_n^w(s)}{\hat{\mathcal{D}}^u(s)} \hat{u}_k \sum_{j=1}^{r_n^a} \frac{\langle \mathbf{b}_k, \boldsymbol{\psi}_{n_j}\rangle_{\boldsymbol{\mathcal{H}}}}{\lambda_n} \boldsymbol{\phi}_{n_j} \tag{12}$$

where

$$\begin{aligned} \hat{\mathcal{D}}_n^w(s) &= \prod_{l\in\mathbb{N},\, l\neq n} \left(1 - \frac{s}{\lambda_l}\right) e^{\mathcal{F}(\frac{s}{\lambda_l}, g)}, \\ \hat{\mathcal{D}}^u(s) &= \prod_{l\in\mathbb{N}} \left(1 - \frac{s}{\lambda_l}\right) e^{\mathcal{F}(\frac{s}{\lambda_l}, g)}, \end{aligned} \tag{13}$$

denote so-called Weierstrass canonical products of genus[3] g of its sequence of zeros $(\lambda_l)_{l\in\mathbb{N}}$ [10]. Herein, $\mathcal{F}(s, g) = 0$ if $g = 0$ or $\mathcal{F}(s, g) = \sum_{j=1}^{g} s^j/j$ if $g \geq 1$. This formulation becomes apparent by considering the relationship between Weierstrass canonical products and entire functions. For any sequence $(\lambda_l)_{l\in\mathbb{N}}$ with genus $g \geq 0$ the products $\hat{\mathcal{D}}_n^w(s)$ and $\hat{\mathcal{D}}^u(s)$ converge and define entire functions whose zeros are exactly $(\lambda_l)_{l\in\mathbb{N},\, l\neq n}$ and $(\lambda_l)_{l\in\mathbb{N}}$.

This Weierstrass factorized representation enables the introduction of a flat output in the operational domain by substituting $\hat{\xi}_k(s) = \hat{u}_k(s)/\hat{\mathcal{D}}^u(s)$, which together with (12) yields

$$\hat{\boldsymbol{w}} = -\sum_{n\in\mathbb{N}} \sum_{k=1}^{N_p} e^{\mathcal{F}(\frac{s}{\lambda_n}, g)} \hat{\mathcal{D}}_n^w(s) \hat{\xi}_k \sum_{j=1}^{r_n^a} \frac{\langle \mathbf{b}_k, \boldsymbol{\psi}_{n_j}\rangle_{\boldsymbol{\mathcal{H}}}}{\lambda_n} \boldsymbol{\phi}_{n_j} \tag{14a}$$

$$\hat{u}_k = \hat{\mathcal{D}}^u(s) \hat{\xi}_k, \quad k = 1, \dots, N_p. \tag{14b}$$

Moreover, note that any entire function can be expanded into a MacLaurin series, i.e.

$$\begin{aligned} {}'\mathcal{D}_n^w(s) &:= e^{\mathcal{F}(\frac{s}{\lambda_l}, g)} \hat{\mathcal{D}}_n^w(s) = \sum_{l\in\mathbb{N}} c_l^w s^l \\ \hat{\mathcal{D}}^u(s) &= \sum_{l\in\mathbb{N}} c_l^u s^l, \end{aligned} \tag{15}$$

with $c_0^w = c_0^u = 1$, which converge for all $s \in \mathbb{C}$. Hence, by taking into account that s is the operational equivalent to time differentiation the state and input parametrizations (14) are equivalent to

$$\boldsymbol{w} = -\sum_{n\in\mathbb{N}} \sum_{k=1}^{N_p} ({}'\mathcal{D}_n^w(\partial_t) \circ \xi_k) \sum_{j=1}^{r_n^a} \frac{\langle \mathbf{b}_k, \boldsymbol{\psi}_{n_j}\rangle_{\boldsymbol{\mathcal{H}}}}{\lambda_n} \boldsymbol{\phi}_{n_j} \tag{16a}$$

$$u_k = \mathcal{D}^u(\partial_t) \circ \xi_k, \quad k = 1, \dots, N_p. \tag{16b}$$

These computations are so far only formal and rely on the convergence of (16). This, however, can in principle be reduced to a problem of trajectory assignment for the flat output taking into account the eigenvalue distribution, which determines the series coefficients in (15).

[3]The smallest positive integer g' for which $\sum_{n\in\mathbb{N}} |a_n|^{-g'} < \infty$ with $a_n \neq 0$, $\lim_{n\to\infty} |a_n| \to \infty$ is denoted as $g + 1$ and g is the genus of the sequence $(a_n)_{n\in\mathbb{N}}$ [10].

Post-print version of the article: J. Schröck, T. Meurer, and A. Kugi, "Motion planning for an elastic Kirchhoff plate", in *Proceedings of the American Control Conference (ACC)*, Montreal, Canada, Jun. 2012, pp. 652–657
The content of this post-print version is identical to the published paper but without the publisher's final layout or copy editing.

B. Convergence analysis

Similar to the treatise in [14] for an Euler-Bernoulli beam and [12] for a diffusion-reaction system with higher-dimensional spatial domain the convergence of $\boldsymbol{w}(t)$ and $u_k(t)$, $k = 1, ..., N_p$ parametrized according to (16) relies on the order and type[4] of ${}'\mathcal{D}_n^w(s)$ and $\hat{\mathcal{D}}^u(s)$. In addition, it is obvious from (16) that necessarily $\xi_k(t) \in C^\infty(\mathbb{R})$. We have the following convergence result.

Theorem 1: Let $(\lambda_n)_{n\in\mathbb{N}}$ be of convergence exponent[5] ν and genus g, then $\hat{\mathcal{D}}^u(s)$ is an entire function of order $\varsigma = \nu$ and genus g. If $\hat{\mathcal{D}}^u(s)$ is of finite type τ, then $u_k(t) = \mathcal{D}^u(\partial_t) \circ \xi_k(t)$ converges uniformly for any $\xi_k(t) \in G_{D,\alpha}(\mathbb{R})$, the Gevrey class[6] of order $\alpha < 1/\varsigma$.

Proof: Since $\hat{\mathcal{D}}^u(s)$ is a Weierstrass canonical product it is an entire function of order equal to the convergence exponent ν of its sequence of zeros $(\lambda_n)_{n\in\mathbb{N}}$ [3, Thm. 2.6.5]. The genus follows from the Hadamard theorem [10, Sec. 4.2]. Moreover, if $\hat{\mathcal{D}}^u(s)$ is of finite type, then there exists a finite $m(\epsilon) \in \mathbb{N}$ s.t. for any $\epsilon > 0$ the coefficients c_l^u of the MacLaurin series expansion satisfy $|c_l^u| \leq [(e\varsigma\tau + \epsilon)/l]^{l/\varsigma}$ for all $l > m(\epsilon)$. Since (14b) is equivalent to $u_k(t) = \sum_{l\in\mathbb{N}} c_l^u \partial_t^l \xi_k(t)$ uniform convergence can be directly deduced by taking into account the bound on c_l^u, the Gevrey condition, and the Cauchy-Hadamard theorem. ■

As is shown in [14], [12] a rather similar argument allows to deduce the convergence of ${}'\mathcal{D}_n^w(\partial_t) \circ \xi_k(t)$ for any $n \in \mathbb{N}$. The convergence of the parametrized Fourier series (16a) can be in addition deduced provided that $\sum_{n\in\mathbb{N}} \sum_{j=1}^{r_n^a} |\sum_{k=1}^{N_p} ({}'\mathcal{D}_n^w(\partial_t) \circ \xi_k) \langle \mathbf{b}_k, \boldsymbol{\psi}_{n_j}\rangle_{\boldsymbol{\mathcal{H}}} / \lambda_n|^2 < \infty$ holds. The latter obviously depends on the actuator type and location. The explicit proof of these claims is subsequently omitted but makes use of the following assumption, which implies the approximate controllability of (7) according to [4, Thm. 4.2.1].

Assumption 2: For all $n \in \mathbb{N}$ the $(r_n^a \times N_p)$-matrix defined by $[\langle \mathbf{b}_1, \boldsymbol{\psi}_{n_j}\rangle_{\boldsymbol{\mathcal{H}}}, \ldots, \langle \mathbf{b}_{N_p}, \boldsymbol{\psi}_{n_j}\rangle_{\boldsymbol{\mathcal{H}}}]_{j=1,\ldots,r_n^a}$ is of rank r_n^a.

The verification of the convergence conditions on the one hand relies on appropriate trajectory assignment for the flat output addressing the Gevrey condition with $\alpha < 1/\varsigma$ and the considered motion planning problem. On the other hand, order and type depend on the zero set of ${}'\mathcal{D}_n^w(s)$ and $\mathcal{D}^u(s)$, which corresponds to the eigenvalue distribution. Both tasks are addressed below.

C. Trajectory assignment for the flat output

The parametrization of the system state directly yields the parametrization of the output (3), i.e.

$$y_i = -\sum_{n\in\mathbb{N}} \sum_{k=1}^{N_p} ({}'\mathcal{D}_n^w(\partial_t) \circ \xi_k) \sum_{j=1}^{r_n^a} \frac{\langle \mathbf{b}_k, \boldsymbol{\psi}_{n_j}\rangle_{\boldsymbol{\mathcal{H}}}}{\lambda_n} c_{n_j,i}, \quad (17)$$

with $c_{n_j,i} = \phi_{1,n_j}(x_i^1, x_i^2)$, $i = 1, ..., N_y$. Obviously, formally prescribing different $\xi_k(t)$ results in different output trajectories $y_i(t)$. Hence, the motion planning problem can be solved indirectly by assigning a suitable desired trajectory $t \mapsto \xi_k^d(t)$, which realizes the desired motion $\boldsymbol{y}^d(t)$. Once $\xi_k^d(t)$ is available the necessary feedforward control directly follows from (16b).

In particular, (17) can be used to realize rest-to-rest motion from $\boldsymbol{y}_s^0 = \boldsymbol{y}(0)$ to $\boldsymbol{y}_s^T = \boldsymbol{y}(T)$ with prescribed transition time T. The corresponding values of the flat output $\boldsymbol{\xi}_s^0 = \boldsymbol{\xi}(0)$ and $\boldsymbol{\xi}_s^T = \boldsymbol{\xi}(T)$ can be directly determined from the output parametrization under steady state conditions, i.e.

$$y_{s,i}^{\{0,T\}} = -\sum_{n\in\mathbb{N}} \sum_{k=1}^{N_p} \xi_{s,k}^{\{0,T\}} \sum_{j=1}^{r_n^a} \frac{\langle \mathbf{b}_k, \boldsymbol{\psi}_{n_j}\rangle_{\boldsymbol{\mathcal{H}}}}{\lambda_n} c_{n_j,i} \quad (18)$$

for $i = 1, \ldots, N_y$, which directly follows from (17) by making use of the final value theorem of Laplace transform. Assumption 2 thereby implies that $\dim \boldsymbol{\xi} = N_p$ independent output trajectories can be assigned. Thus, let $N_y = N_p$ and let the conditions of Theorem 1 hold, then (18) represents a linear system of equations for $\boldsymbol{\xi}_s^{\{0,T\}}$. Moreover, it is obvious that the connection of $\boldsymbol{\xi}_s^0$ and $\boldsymbol{\xi}_s^T$ requires $\boldsymbol{\xi}(t)$ to be locally non–analytic at $t \in \{0, T\}$, i.e. $\boldsymbol{\xi}(0) = \boldsymbol{\xi}_s^0$, $\boldsymbol{\xi}(T) = \boldsymbol{\xi}_s^T$ with $\partial_t^n \boldsymbol{\xi}(t) = 0$ at $t = \{0, T\}$ for all $n \geq 1$. In view of Theorem 1 this requires $\alpha > 1$ or $\varsigma < 1$.

D. Finite-dimensional approximation and a graphical convergence indicator

It is obvious that in general no analytical solution to the operator eigenvalue problem is available. Hence, to address the explicit (approximate) computation of the eigenvalue distribution, the weak formulation (4) can be utilized to determine a finite-dimensional approximation of the equations of motion in the sense of weighted residuals [11]. For this, consider the Fourier series (9) truncated at an arbitrary finite integer $m \in \mathbb{N}$, i.e.

$$\boldsymbol{w}^m = \sum_{n=1}^{m} \sum_{j=1}^{r_n^a} \langle \boldsymbol{w}, \boldsymbol{\psi}_{n_j}\rangle_{\boldsymbol{\mathcal{H}}} \boldsymbol{\phi}_{n_j} = \sum_{n=1}^{m} \sum_{j=1}^{r_n^a} q_{n_j} \boldsymbol{\phi}_{n_j}, \quad (19)$$

where $q_{n_j}(t) := \langle \boldsymbol{w}(t), \boldsymbol{\psi}_{n_j}\rangle_{\boldsymbol{\mathcal{H}}}$. By selecting the test functions $\zeta(x^1, x^2) \in \mathcal{V}$ equal to the set of basis functions $((\boldsymbol{\psi}_{n_j})_{j=1,\ldots,r_n^a})_{n=1}^m$, the evaluation of (4) directly yields a finite-dimensional model of the considered patch-actuated cantilevered plate in the form

$$\begin{aligned} M\partial_t^2 \boldsymbol{q} + D\partial_t \boldsymbol{q} + K\boldsymbol{q} &= B\boldsymbol{u} \\ \boldsymbol{y} &= C\boldsymbol{q} \end{aligned} \quad (20)$$

with $\boldsymbol{q}^T(t) = [q_{1_1}(t), ..., q_{1_{r_1^a}}(t), ..., q_{m_1}(t), ..., q_{m_{r_m^a}}(t)]$, $\boldsymbol{u}^T(t) = [u_1(t), \ldots, u_{N_p}(t)]$, $y_i = w_1^m(x_i^1, x_i^2)$, $i = 1, ..., N_y$ and the symmetric $\mathbb{R}^{N\times N}$, $N = \sum_{n=1}^m r_n^a$ matrices M, D, and K as well as $B \in \mathbb{R}^{N\times N_p}$, $C \in \mathbb{R}^{N_y\times N}$. Note that a proper evaluation of the matrix elements requires that the basis functions fulfill (2a).

[4]For a definition of these notions for entire functions consult [3], [10].

[5]The infimum ν of positive numbers ν' such that $\sum_{n\in\mathbb{N}} |a_n|^{-\nu'} < \infty$ with $a_n \neq 0$ and $\lim_{n\to\infty} |a_n| \to \infty$ is called the convergence exponent of the sequence $(a_n)_{n\in\mathbb{N}}$ [10].

[6]The function $f(t) \in C^\infty(\mathbb{R})$ is in $G_{D,\alpha}(\mathbb{R})$ if there exist D, $\alpha > 0$ such that $\sup_{t\in\mathbb{R}} |\partial_t^n f(t)| \leq D^{n+1}(n!)^\alpha$ for any $n \in \mathbb{N}$. $f(t)$ is entire if $\alpha < 1$, analytic if $\alpha = 1$, and non-analytic if $\alpha > 1$.

Post-print version of the article: J. Schröck, T. Meurer, and A. Kugi, "Motion planning for an elastic Kirchhoff plate", in *Proceedings of the American Control Conference (ACC)*, Montreal, Canada, Jun. 2012, pp. 652–657
The content of this post-print version is identical to the published paper but without the publisher's final layout or copy editing.

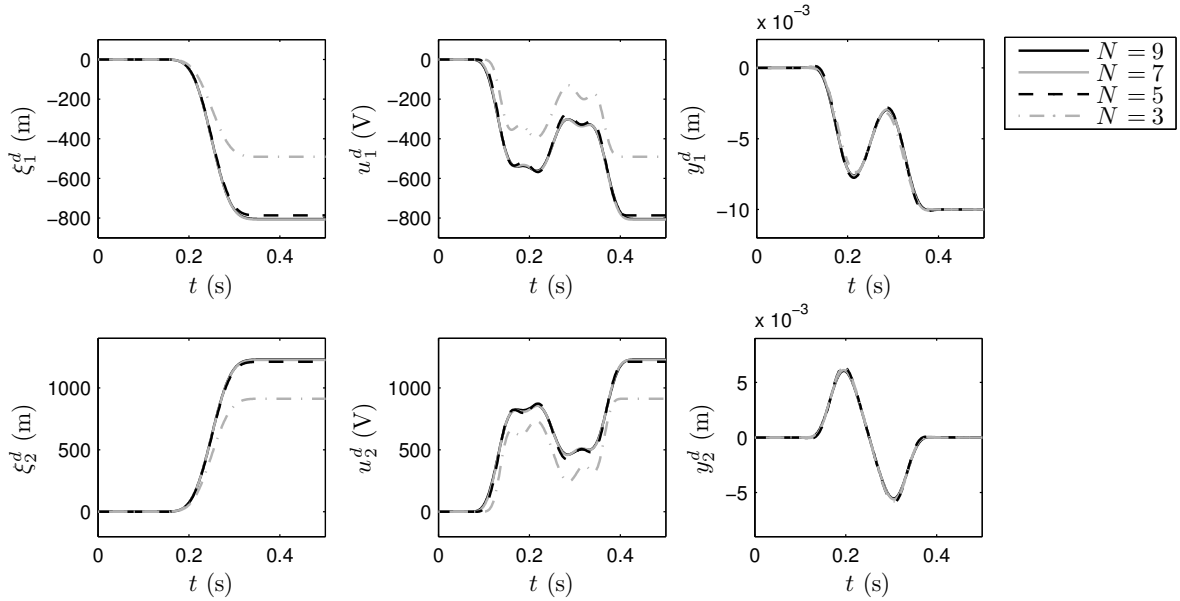

Fig. 2: Convergence of the flatness-based parametrizations (16) for different numbers N of basis functions: trajectories for the flat outputs $\xi_1^d(t)$, $\xi_2^d(t)$ (left), voltage input $u_1^d(t)$, $u_2^d(t)$ (center), output trajectories $y_1^d(t)$, $y_2^d(t)$ (right).

Based on (20), the state and input parametrizations can be explicitly evaluated by replacing $\mathbb{N}$ with m and making use of the solution of the algebraic eigenproblem

$$(\overline{M}\lambda + \overline{K})\boldsymbol{\theta} = 0, \tag{21}$$

where $\overline{M} = \left(\begin{smallmatrix} D & M \\ M & 0 \end{smallmatrix}\right)$ and $\overline{K} = \left(\begin{smallmatrix} K & 0 \\ 0 & -M \end{smallmatrix}\right)$ are symmetric $2N \times 2N$ matrices. With this, on the one hand a very efficient computational evaluation is achieved and on the other hand a high-order approximation can be used to deduce a graphical convergence indicator. For this, observe that the convergence exponent ν of a sequence with countable index set equals the order of its counting function [10, Sec. 3.2]. Let $\mathfrak{n}(r)$ denote the counting function of $(\lambda_n)_{n\in\mathbb{N}}$, i.e. $\mathfrak{n}(r) = \#\{\lambda_n,\, n \in \mathbb{N} : |\lambda_n| \leq r\}$, this yields $\nu = \limsup_{r\to\infty} \log \mathfrak{n}(r)/\log(r)$. Hence, the graph $\log \mathfrak{n}(r)/\log(r)$ can be considered as an indicator for ν and hence the order ς provided that a sufficiently large number of eigenvalues can be numerically determined by making use of (21).

Nevertheless, it should be pointed out that also divergent parametrizations can be used for the solution of the motion planning problem as is shown in [12].

V. Simulation results

In the following, simulation results are presented by making use of the presentation in Section IV-D for the determination of the feedforward control to realize rest-to-rest motions for the considered Kirchhoff plate.

For this, the spatial actuator characteristics are assumed to satisfy $\Lambda_k(x^1, x^2) = [h(x^1 - x_k^1) - h(x^1 - x_k^1 - L_k^1)] \times [(h(x^2 - x_k^2) - h(x^2 - x_k^2 - L_k^2)]$, where $h(\cdot)$ denotes the Heaviside function and the rectangle $(x_k^1, x_k^1 + L_k^1) \times (x_k^2, x_k^2 + L_k^2)$ represents the spatial extension of the k-th patch actuator.

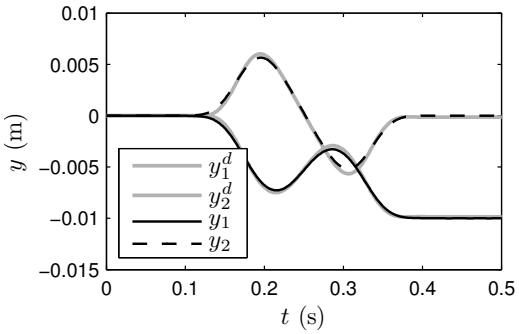

Fig. 3: Comparison between the desired output trajectories $y_k^d(t)$ (light gray curves) and the obtained output trajectories $y_k(t)$ (black curves), $k = 1, 2$.

The basis functions for the evaluation of (20) are chosen as the eigenvectors of an undamped orthotropic cantilevered plate and are determined using finite elements.

An orthotropic plate of dimensions $L^1 = 0.6$ m, $L^2 = 0.3$ m is considered with $\rho^c = 1.5$ kg/m^2, $\gamma^c = 1.5$ kg/(sm^2) and material parameters $I_1^c = I_2^c = 1.45$ kNm, $I_3^c = 0.34$ kNm, $I_4^c = 1.56$ kNm. Two identical pairs ($N_p = 2$) of piezoelectric patch actuators of dimensions $L_1^1 = 0.085$ m, $L_1^2 = 0.057$ m are located at $(x_1^1, x_1^2) = (0.023, 0.02)$ m, $(x_2^1, x_2^2) = (0.023, 0.223)$ m with $\rho^p = 1.6$ kg/m^2, $\gamma^p = 2.5$ kg/(sm^2), $I_1^p = I_2^p = 3$ kNm, $I_3^p = 2$ kNm, $I_4^p = 6$ kNm, and $\Gamma_1^p a_1^{11} = \Gamma_2^p a_1^{22} = -0.005$ As/m. The inputs $u_k(t)$ correspond to the voltages applied to the actuators.

The considered motion planning problem is motivated by an adaptive wing configuration to influence the surrounding

Post-print version of the article: J. Schröck, T. Meurer, and A. Kugi, "Motion planning for an elastic Kirchhoff plate", in *Proceedings of the American Control Conference (ACC)*, Montreal, Canada, Jun. 2012, pp. 652–657
The content of this post-print version is identical to the published paper but without the publisher's final layout or copy editing.

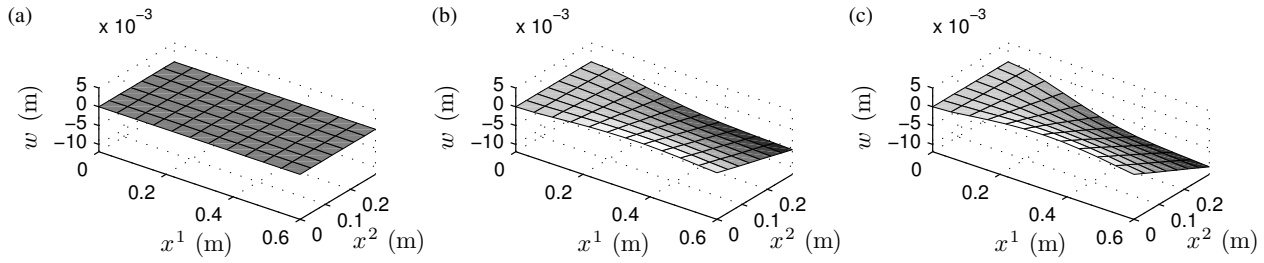

Fig. 4: Deflection of the patch-actuated plate at different instances of time: (a) $t = 0$ s, (b) $t = 0.25$ s, (c) $t = 0.5$ s.

flow field. For this, the system output is defined by the deflection at the free corners of the plate, i.e. $N_y = 2$, and

$$y_1 = w|_{(x^1,x^2)=(L^1,0)}, y_2 = w|_{(x^1,x^2)=(L^1,L^2)}.$$

The rest-to-rest trajectory for the trailing edge of the wing is determined by the desired initial and final values $y^0_{s,1} = y^T_{s,1} = 0$ for $y_1(t)$ and $y^0_{s,2} = 0$ and $y^T_{s,2} = -0.01$ m for $y_2(t)$. The non-analytic transition function

$$\xi^d_k(t) = \begin{cases} \xi^0_{s,k}, & t < 0 \\ \xi^0_{s,k} + \frac{\xi^T_{s,k}}{2}\left[1+\tanh\left(\frac{2\left(\frac{2t}{T}-1\right)}{\left(\frac{4t}{T}\left(1-\frac{t}{T}\right)\right)^\sigma}\right)\right], & t \in [0,T] \\ \xi^0_{s,k} + \xi^T_{s,k}, & t > T \end{cases}$$

of Gevrey order $\alpha = 1 + 1/\sigma$ is assigned to the flat output $\xi_k(t)$, where $\sigma = 1.9$ determines the slope, $T = 0.5$ s denotes the transition time, and $\xi^0_{s,k}$, $\xi^T_{s,k}$ represent initial and final values determined from (18).

The desired trajectories for the flat output and numerical evaluations of the input and output parametrization (16b), (17) are shown in Figure 2 for different numbers N of basis functions. The numerical results show that all eigenvalues are mutually disjoint. Obviously, rather fast convergence is obtained with the input voltages evolving in rather non-trivial fashion but at realistic amplitudes. The tracking behavior is evaluated in Figure 3 by comparing the desired output with the output obtained by applying the feedforward control with $N = 9$ to the simulation model corresponding to (20) with $N = 11$. Snapshots of the evolving deflection profile are depicted in Figure 4 for different instances of time. These results clearly confirm the applicability and high tracking performance of the proposed motion planning and feedforward control design.

VI. Conclusion and Outlook

In this contribution, a flatness-based approach for motion planning and feedforward control is presented for the example of an orthotropic cantilevered Kirchhoff plate with spatially varying coefficients resulting from distributed patch actuators. For this, the spectral representation of the equations of motion is utilized to systematically determine a flatness-based state and input parametrization. The convergence of the parametrization depends on the eigenvalue distribution and properties of the flat output. By making use of a weighted-residual approach an efficient realization of the feedforward controller is available. Simulation results for the example of high-speed rest-to-rest motion for an adaptive wing illustrate the applicability and tracking performance of the proposed concept.

Current work is dedicated to the experimental validation of the proposed design approach.

References

[1] H. T. Banks, R. C. H. Smith, and Y. Wang, *Smart Material Structures: Modelling, Estimation and Control*. Paris: John Wiley & Sons, 1996.

[2] J. Becker and T. Meurer, "Feedforward Tracking Control for Non–Uniform Timoshenko Beam Models: Combining Differential Flatness, Modal Analysis and FEM," *Z. Angew. Math. Mech. (ZAMM)*, vol. 87, no. 1, pp. 37–58, 2007.

[3] R. P. Boas, *Entire Functions*. New York: Academic Press Inc., 1954.

[4] R. F. Curtain and H. J. Zwart, *An Introduction to Infinite-Dimensional Linear Systems Theory*. New York: Springer, 1995.

[5] M. Fliess, J. Lévine, P. Martin, and P. Rouchon, "Flatness and defect of non–linear systems: introductory theory and examples," *Int. J. Control*, vol. 61, pp. 1327–1361, 1995.

[6] M. Fliess, H. Mounier, P. Rouchon, and J. Rudolph, "Systèmes linéaires sur les opérateurs de Mikusiński et commande d'une poutre flexible," *ESAIM Proc.*, vol. 2, pp. 183–193, 1997.

[7] B. Guo, "Riesz basis property and exponential stability of controlled Euler-Bernoulli beam equations with variable coefficients," *SIAM Journal on Control and Optimization*, vol. 40, no. 6, pp. 1905–1923, 2002.

[8] B.-Z. Guo and H. Zwart, "Riesz spectral systems," Faculty of Mathematical Sciences, University of Twente, The Netherlands, Memorandum 1594, 2001.

[9] A. W. Leissa, *Vibration of Plates*. NASA SP-160, US Government Printing Offices, 1969.

[10] B. Levin, *Lectures on Entire Functions*. Providence, Rhode Island: American Mathematical Society, 1996.

[11] L. Meirovitch, *Principles and Techniques of Vibrations*. New Jersey: Prentice Hall, 1997.

[12] T. Meurer, "Flatness–based Trajectory Planning for Diffusion–Reaction Systems in a Parallelepipedon — A Spectral Approach," *Automatica*, vol. 47, no. 5, pp. 935–949, 2011.

[13] T. Meurer and A. Kugi, "Inversion–Based Transient Shaping of a Piezo–Actuated Plate: Motion Planning and Feedforward Control," in *Proc. (CD–ROM) 4th IFAC Symposium on Mechatronic Systems*, Heidelberg (D), Sep. 12–14 2006, pp. 169–174.

[14] T. Meurer, J. Schröck, and A. Kugi, "Motion planning for a damped euler-bernoulli beam," in *Proc. 49th IEEE Conference on Decision and Control (CDC)*, Atlanta (USA), Dec. 15-17 2010, pp. 2566–2571.

[15] T. Meurer, D. Thull, and A. Kugi, "Flatness–based tracking control of a piezoactuated Euler–Bernoulli beam with non–collocated output feedback: theory and experiments," *Int. J. Contr.*, vol. 81, no. 3, pp. 475–493, 2008.

[16] J. Schröck, T. Meurer, and A. Kugi, "Motion planning for an adaptive wing structure with macro-fiber composite actuators," ser. SPIE Conference Series, vol. 7362, no. 1, Dresden (D), May 4-6 2009, p. 73621H (11 pages).

[17] F. Woittennek and J. Rudolph, "Motion planning for a circular elastic plate," *Proc. Appl. Math. Mech. (PAMM)*, vol. 4, pp. 149–150, 2004.

Post-print version of the article: J. Schröck, T. Meurer, and A. Kugi, "Motion planning for an elastic Kirchhoff plate", in *Proceedings of the American Control Conference (ACC)*, Montreal, Canada, Jun. 2012, pp. 652–657
The content of this post-print version is identical to the published paper but without the publisher's final layout or copy editing.